Cardiovascular Research (2016) **109**, 260–271
doi:10.1093/cvr/cvv270

Loss of plakoglobin immunoreactivity in intercalated discs in arrhythmogenic right ventricular cardiomyopathy: protein mislocalization versus epitope masking

Sebastian Kant[1], Claudia A. Krusche[1], Anna Gaertner[2], Hendrik Milting[2], and Rudolf E. Leube[1]*

[1]Institute of Molecular and Cellular Anatomy, RWTH Aachen University, Wendlingweg 2, Aachen 52074, Germany; and [2]Herz- und Diabeteszentrum NRW, Klinik für Thorax- und Kardiovaskularchirurgie, Erich und Hanna Klessmann-Institut für Kardiovaskuläre Forschung und Entwicklung, Bad Oeynhausen, Germany

Received 23 December 2014; revised 19 November 2015; accepted 27 November 2015; online publish-ahead-of-print 16 December 2015

Time for primary review: 37 days

Aims To examine the relevance and cause of reduced plakoglobin IF in intercalated discs for arrhythmogenic right ventricular cardiomyopathy (ARVC) and ARVC-like disease in mouse and human.

Methods and results Normalized semi-quantitative IF measurements were performed in a standardized format in desmoglein 2-mutant mice with an ARVC-like phenotype ($n = 6$) and in cardiac biopsies from humans with ARVC and non-ARVC heart disease ($n = 10$). Reduced plakoglobin staining was detectable in ARVC only with one antibody directed against a defined epitope but not with three other antibodies reacting with different epitopes of plakoglobin.

Conclusions Reduced plakoglobin staining in intercalated discs of heart tissue from human ARVC patients and in a murine ARVC model is caused by alterations in epitope accessibility and not by protein relocalization.

Keywords Wnt signalling • Armadillo repeat • β-catenin • Desmosome • Area composita

1. Introduction

Arrhythmogenic right ventricular cardiomyopathy (ARVC) also referred to as arrhythmogenic cardiomyopathy (AC) and arrhythmogenic right ventricular dysplasia (ARVD) is an inherited heart disease with a prevalence of 1:2000–1:10000 (http://www.orpha.net). Since it has been considered to be a disease of the right ventricle, the revised task force criteria focus primarily on right ventricular pathology.[1] Despite these criteria, diagnosis of ARVC has remained difficult, especially in light of the growing evidence for biventricular and even predominant left ventricular involvement.[2] This paradigm shift, which is paralleled by findings in murine ARVC models,[3–6] has posed additional problems in the reliable diagnosis of ARVC.

Improvements in genetic testing have shown that mutations in genes encoding desmosomal proteins are the most common genetic alterations in ARVC, which has been referred to as a disease of the desmosome.[7,8] Most mutations have been identified in the plakophilin 2 gene, followed by mutations in the genes encoding desmoglein 2 and desmoplakin and the fewest mutations in the genes coding for plakoglobin, desmocollin 2 and the desmosome-associated intermediate filament protein desmin.[9–12] In addition, mutations in the non-desmosomal proteins transforming growth factor β3, ryanodine receptor 2, transmembrane protein 43, phospholamban, lamin, and titin have been reported with highly variable prevalence in different populations.[13,14] Furthermore, the genes in four other ARVC-causing loci (ARVC 3, 4, 6, and 7) have not been identified to date.[11] Although the detection of pathogenic mutations is a major criterion in the diagnosis of ARVC, all known mutations account only for <65% of ARVC cases.[8–10]

Given the above-mentioned uncertainties in ARVC diagnosis, additional diagnostic criteria have been searched for and proposed. Among them is the reduction of plakoglobin at the intercalated disc as determined by IF microscopy of sectioned myocardial biopsies.[15] Plakoglobin localization was examined in this study in biopsies of 11 ARVC patients, 8 of which had mutations in desmosomal genes. It was compared with 14 biopsies of patients with heart disease other than ARVC

* Corresponding author. Tel: +49 2418089107; fax: +49 2418082508, E-mail: rleube@ukaachen.de

and 10 healthy controls. A reduction of plakoglobin localization in intercalated discs was detected in all ARVC samples but in none of the controls. These findings were corroborated by blinded analyses of another sample series.[15] Since then reduced plakoglobin localization at intercalated discs of ARVC patients was reported repeatedly using either IF[16–18] or immunohistochemistry.[19–21] In some studies, however, reduced plakoglobin immunoreactivity was observed in a considerable number of patients with heart diseases other than ARVC.[19,22] Even more, some authors could not detect a reduction in intercalated disc localization of plakoglobin in comparison to control groups using either IF[23] or immunohistochemistry.[24] Some of the observed differences may be related to technical issues, since quantification of IF and immunohistochemical reactions is rather challenging and requires careful controls and standardization.

To resolve the existing discrepancies, we designed a cross-species study in which variables were reduced as much as possible by adjusting immunosignals to within the dynamic detection range, by normalization of recordings using control reactions in the same tissue sections and by recording entire data sets with identical settings in single sessions. In this way, we were able to derive highly reproducible results in a murine model of ARVC and in human ARVC patients using different plakoglobin antibodies. Our results show that the surmised reduction of plakoglobin localization in intercalated discs is most likely caused by differential epitope accessibility. The implications of these findings are discussed with respect to the proposed function of plakoglobin in the pathogenesis of ARVC.[25–27]

2. Methods

2.1 Tissue acquisition and IF microscopy

Mice were housed in the central animal facility of the University Hospital of RWTH Aachen University. The animals were fed standard rodent lab diet (Sniff) and had free access to food and water. The animal experiments were approved by the Landesamt für Natur, Umwelt und Verbraucherschutz (LANUV) Nordrhein-Westfalen under the reference number 8.87–50.10.37.09.114. This governmental institution is bound to follow the German law and the guidelines from Directive 2010/63/EU when approving animal test proposals. The characteristics of the used mouse strain have been described previously (supplementary data in Ref. 4). Homozygous mutant mice and wild-type controls were killed at the age of 2 and 12 weeks by cervical dislocation. Hearts were dissected, cut in half, and fixed in 4% buffered formaldehyde overnight. The tissues were then dehydrated using a graded isopropanol series and were embedded in paraffin according to standard protocols. It was subsequently cut into 5 μm thick sections, deparaffinized, and subsequently rehydrated. For epitope retrieval, sections were transferred into 10 mM citrate buffer (pH 6.0) and heated for 3 min at maximum pressure in a pressure cooker. A mixture of primary antibodies diluted in PBS containing 1.5% (w/v) BSA was applied over night at 4°C, and unbound antibodies were removed by two times washing for 10 min in TBST buffer containing 50 mM Tris/HCl (pH 7.5), 0.05% (v/v) Tween 20, and 0.3 M NaCl. Secondary antibodies were diluted 1:500 in 1.5% (w/v) BSA/PBS and were applied for 1 h in the dark at room temperature. Two 10 min TBST washing steps followed and unspecific background staining was quenched by 30 min incubation in quenching solution [0.1% (w/v) Sudan black B (Merck) dissolved in 70% ethanol]. After three times washing with TBST for 10 min, sections were counterstained with DAPI and mounted in Mowiol 4–88-based mounting medium (Roth).

Human myocardial tissue was obtained from patients with end-stage heart failure and from donor hearts rejected due to technical reasons within the heart transplant program at the Herz- und Diabeteszentrum NRW. End-stage heart failure was caused by dilated cardiomyopathy (DCM) or ARVC. Diagnosis of ARVC was based on clinical and genetic parameters that have been defined by the task force.[1] This classification distinguishes six categories concerning global or regional dysfunction and structural alterations (I), tissue characterization of wall (II), repolarization abnormalities (III), depolarization abnormalities (IV), arrhythmias (V), and family history (VI). Each category comprises several major and minor criteria. *Table 1* lists all the major and minor criteria within each category that were fulfilled in the different patients showing that each fulfils the requirement for definite ARVC diagnosis, i.e. at least two major criteria from different categories. Of note, the mutations in patients 1, 2, 3, 6, 7, 8, and 10 have been described as pathogenic in earlier reports.[28–31] Some are also listed as pathogenic in OMIM (http://www.ncbi.nlm.nih.gov/omim; patients 2, 8 and 10) and some have been shown to encode either non-functional proteins (patient 6),[30] severely truncated polypeptides (patient 7), or slightly truncated polypeptides (patients 1, 2, 3).

Heart tissue was prepared immediately after explantation and cryoconserved at −80°C until usage. Patients gave informed consent to the use of their explanted hearts, the human study conformed to the declaration of Helsinki, and approval was given by an ethics review board. Eight micrometre thick cryosections were prepared and dried at room temperature for 30 min. Afterwards sections were fixed in pre-cooled acetone for 10 min at 4°C and rehydrated in PBS. A mixture of primary antibodies diluted in 1.5% (w/v) BSA/PBS was applied over night at 4°C, and unbound antibodies were removed by two 10 min washes in PBS. Secondary antibodies diluted in PBS containing 1.5% (w/v) BSA were applied for 1 h at room temperature. Two times washing in PBS followed and sections were counterstained with DAPI prior to mounting.

The following primary antibodies were used: polyclonal antibodies from rabbit against desmocollin 2 (Progen, 610120; 1:1000 for human tissues), histone H3 (Abcam, ab1791; 1:1500 for murine tissues), β-catenin (Sigma, C2206; 1:7000 for human tissues; 1:4000 for murine tissues), N-Cadherin (Abcam, ab12221; 1:3000 for human tissues, 1:1500 for murine tissues), and Dsg2 (affinity-purified Dsg2 IC;[32] 1:3000 for human tissues, 1:1000 for murine tissues), polyclonal antibodies from goat against the carboxyterminus of plakoglobin (Santa Cruz, C0806; 1:1000 for human tissues, 1:150 for murine tissues), polyclonal antibodies from guinea pig against the aminoterminal part of plakoglobin (Progen, GP57, 1:500) and desmoplakin (Progen, DP-1; 1:5000 for human tissues, 1:2000 for murine tissues) and murine monoclonal antibodies against plakophilin 2 [Progen, PP2/86 cell culture supernatant (for epitope mapping, see Ref. 33); 1:500 for human tissues, 1:25 for murine tissues], a circumscribed epitope in the aminoterminal part of plakoglobin [Sigma, clone 15F11 ascites, P8087 (for epitope mapping, see Ref. 34); 1:30000 for human tissues, 1:20000 for murine tissues], and a carboxyterminal epitope of plakoglobin [Progen, clone PG5.1 (for epitope mapping, see Ref. 35); cell culture supernatant 1:30 for murine tissues; purified antibody 1:450 for human tissues]. Secondary antibodies were Alexa488-conjugated goat-anti-rabbit and goat-anti-mouse (Invitrogen, A-11070 and A-110029, respectively), Alexa555-conjugated goat-anti-guinea pig (Invitrogen, A-21435; used on human samples), Cy3-conjugated goat-anti-guinea pig (Dianova, 106–166–003; used on murine samples), and Dylight488-conjugated rabbit-anti-goat (KPL, 072–03–13–06). All secondary antibodies were diluted 1:500. IF staining was always performed simultaneously for an entire test group using identical antibody mixtures for each section. The IF staining was then recorded in a single session using a confocal laser scanning microscope (LSM 710 DUO, Zeiss). To avoid overexposure, laser intensity and detector sensitivity were adjusted to the dynamic detector range using the brightest immunoreaction in wild-type control sections. Lasers were pre-warmed for 1 h prior to the adjustment to further reduce the possibility of variations in illumination intensity during recording. Subsequent image recording was done without any further adjustments in a single run. The fluorescence of the internal reference staining was used to select a suitable region for unbiased recording of the sought-after fluorescence intensity.

Table 1 Clinical and genetic characteristics of ARVC patients

Patient	Gender Age	Mutation	ARVC major criteria[a]	ARVC minor criteria[a]	ARVC task force classification[b]	Additional information
Cohort 1						
1	Male 62 years	• *PKP2* heterozygous c.2176C>T[28,29] p.Q726X	• ϵ-Waves in V1–V3 [IV] • Identification of a pathogenic mutation in the patient [VI] • ARVC confirmed pathologically at autopsy in a first-degree relative [VI]	• >50 to 65% residual myocytes with fibrous replacement of the RV[c] [II] • inverted T-waves V4–V6 [III]	2 major 2 minor → definite diagnosis	Right ventricular dilatation (RVEDD = 42 mm); sudden cardiac death due to suspected ARVC in a first-degree relative
2	Male 65 years	• *PKP2* heterozygous c.1803delC[29] p.D601E*fs* • *CTNNB1* heterozygous c.1090C>G p.Q364E	• <50% residual myocytes with fibrous replacement of the RV[c] [II] • Inverted T-waves in V1–V3 at age >14 years [III] • Identification of a pathogenic mutation [VI]		3 major 0 minor → definite diagnosis	Right ventricular dilatation (RVEDD = 65 mm)
3	Female 61 years	• *DSC2* homozygous c.1912_1917delAGAA[29] p.Q638L*fs*	• Right ventricular dilatation (RVEDD = 54 mm) and dyskinesia[d] [I] • <50% residual myocytes with fibrous replacement of the RV[c] [II] • Inverted T-waves in V1–V3 at age >14 years [III] • Identification of a pathogenic mutation [VI]	• Sudden cardiac death <35 years in a first-degree relative due to suspected ARVC [VI]	4 major 0 minor → definite diagnosis	Left ventricular dilatation
4	Male 24 years	• Unknown	• Right ventricular dilatation (RVEDD = 52 mm) and global dyskinesia[d] [I] • <50% residual myocytes with fibrous replacement of the RV[c] [II] • Inverted T-waves in V1–V3 at age >14 years [III] • ϵ-waves in V1–V3 [IV]		4 major 0 minor → definite diagnosis	
5	Male 51 years	• *CDH2* heterozygous c.254G>C p.G85A	• Right ventricular dilatation (RVEDD = 68 mm) and dyskinesia[d] [I] • <50% residual myocytes with fibrous replacement of the RV[c] [II]		2 major 0 minor → definite diagnosis	
Cohort 2						
6	Female 16 years	• *DES* heterozygous c.347A>G[29,30] p.N116S	• Right ventricular dilatation (RVEDD = 40 mm) and aneurysm[d] [I] • Identification of a pathogenic mutation [VI]		2 major 0 minor → definite diagnosis	
7	Male 60 years	• *PKP2* heterozygous c.658C>T[29] p.Q220X	• Right ventricular dilatation (RVEDD = 58 mm) and aneurysm[d] [I] • Identification of a pathogenic mutation [VI]		2 major 0 minor → definite diagnosis	Asynchronous RV contraction
8[e]	Male 49 years	• *PKP2* heterozygous c.2146–1G>C[31] (splice defect)	• Right ventricular dilatation (RVEDD = 45 mm) and dyskinesia[d] [I] • <50% residual myocytes with fibrous replacement of the RV[c] [II] • Identification of a pathogenic mutation [VI]	• Sudden cardiac death <35 years in a first-degree relative due to suspected ARVC [VI]	3 major 0 minor → definite diagnosis	Left ventricular dilatation and regional akinesia

9	Female 52 years	• Unknown	• Right ventricular dilatation (RVEDD = 63 mm) and regional akinesia[d] [I] • ϵ-waves in V1–V3 [IV]	• Inverted T-waves in V4–V6 [III]	2 major 1 minor → definite diagnosis
10	Female 31 years	• *PKP2* heterozygous c.2146−1G>C[31] (splice defect); c.1138G>A p.E380K; c.1114G>C p.A372P • *RYR2* heterozygous c.4069G>A p.D1357N • *TTN* heterozygous c.75682A>G p.K25228E	• Right ventricular dilatation (RVEDD = 62 mm) and dyskinesia[d] [I] • <50% residual myocytes with fibrous replacement of the RV[e] [II] • Identification of a pathogenic mutation [VI]	• Sudden cardiac death <35 years in a first-degree relative due to suspected ARVC [VI]	3 major 0 minor → definite diagnosis

[a]Revised task force criteria and [b]disease classification according to Marcus *et al.*[1]
[c]In an adaptation to Marcus *et al.*,[1] percentage of residual myocytes with fibrotic replacement was estimated by visual inspection of the right ventricular free wall in surgically removed hearts (see also Supplementary material online, *Figure S4*).
[d]Since PLAX RVOT and PSAX RVOT values were not available, RVEDD was used for assessment of RV dilation.
[e]Patient was also diagnosed to have non-obstructive hypertrophic cardiomyopathy. The reason for this may have been that the patient was an avid cyclist.

For quantification of IF signal intensity of intercalated discs, regions of interest (ROIs) were first defined using a Fiji script applied on either anti-N-cadherin or anti-desmoplakin IF images as internal references. The fluorescence images of the references were transformed into binary pictures using the otsu background algorithm from Fiji. All areas showing a signal were segmented and saved as ROI files. The segmented ROI files were then superimposed on the original images (*Figure 1*). The fluorescence intensities were measured within the ROIs for each fluorescence channel in the original images, and their ratios were then calculated to derive relative intensity averages for all ROIs of each animal. These results were then used for further statistical analysis.

To prepare figures, representative images were selected, and the contrast was linearly enhanced in the same way for all images within each quantification series. Afterwards images were transformed from 16-bit colour depth to 8-bit colour depth.

2.2 Statistical analysis

All results are presented as scatter dot plots with median and inter-quartile range. Since all experimental groups were too small to be tested positive for Gaussian distribution with the D'Agostino and Pearson omnibus normality tests, non-parametric statistical tests were used. Statistical analyses comparing two groups with each other were done with the two-tailed Mann–Whitney test using 95% CIs. Statistical analyses comparing three groups were accomplished by the Kruskal–Wallis test together with the Dunns *post hoc* test using 95% CIs. All statistical analyses were performed with GraphPad PRISM.

3. Results

3.1 Double fluorescence microscopy is a suitable method to quantify protein localization in intercalated discs

To shed light on the inconsistent observations on intercalated disc localization of desmosomal proteins in ARVC, we established a reliable semi-quantitative immunolocalization procedure. In contrast to previous attempts, we calibrated the immunoreactions to an endogenous standard to account for variables such as tissue preservation, tissue fixation, regional tissue properties, and sectional planes. Furthermore, we used image analysis tools to avoid investigator-specific bias.

We first determined the non-saturating levels of primary antibody concentrations. Dilution series of antibodies were tested to define the dynamic range of antibody concentrations. Signals within this range allow a direct correlation to local epitope levels. These assays were performed for all primary antibodies on wild-type murine and healthy human cardiac tissue samples. For double labelling, concentrations were then chosen that were at least one order of magnitude below the saturation level of the respective IF signals.

In a first set of experiments, we tested candidate epitopes to serve as endogenous standards for normalization of IF reactions. To this end, we examined the fluorescence staining against the adherens junction protein N-cadherin, which has been shown to be unperturbed in ARVC[15,18,20,24] and has been used as a quality criterion in the past,[15] and compared it with the desmosomal protein desmoplakin. *Figure 1* shows the results for a co-immunostaining in wild-type and desmoglein 2-mutant heart tissues. In addition to the specific intercalated disc staining (arrows), however, autofluorescent red blood cells were also detected (arrowheads). Next, Fiji software was used to automatically segment intercalated disc regions. The segmentation was efficient as seen in the merged images of *Figure 1* (areas encircled in white) with

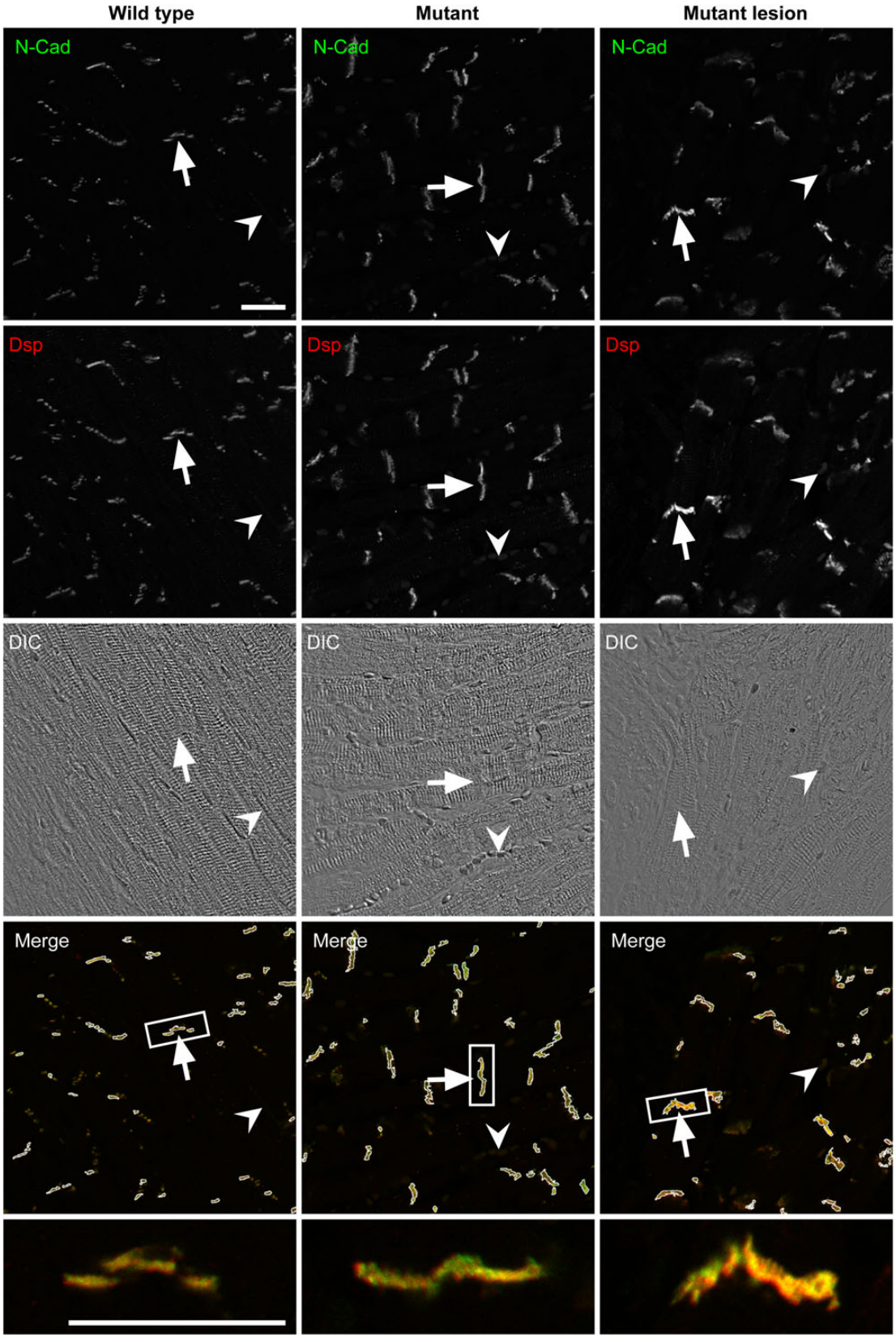

Figure 1 Co-localization of N-cadherin and desmoplakin in intercalated discs is indistinguishable between wild-type and desmoglein 2 mutant hearts. Double IF microscopy [top rows; corresponding differential interference contrast images below (DIC)] detecting N-cadherin (N-Cad) with desmoplakin (Dsp) in 12-week-old wild-type and desmoglein 2-mutant hearts far away (mutant) or near a myocardial lesion (mutant lesion). Note the localization of both antigens at intercalated discs irrespective of genotype (white arrows). Non-specific autofluorescence was observed in erythrocytes within blood vessels (white arrowheads). The results of automated segmentation are shown as encircled regions. Note that non-specific autofluorescence is excluded from the segmented ROIs in most instances. Enlargements of boxed double fluorescence images are shown in the bottom panels. Size bars, 20 μm.

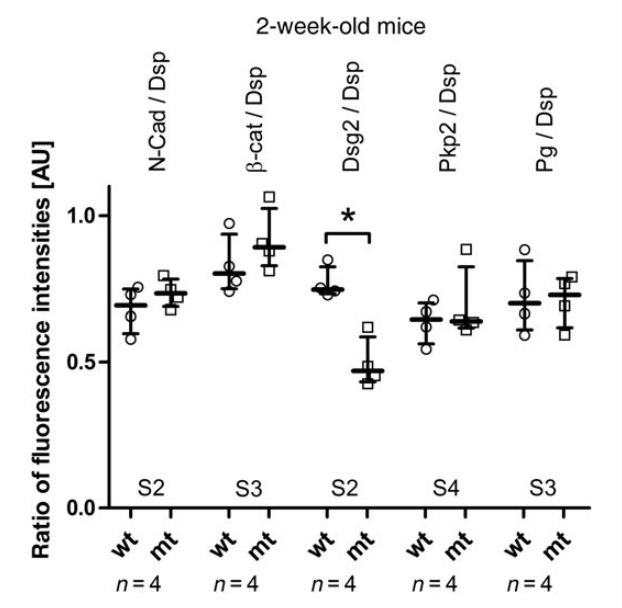

Figure 2 β-Catenin, plakophilin 2, and plakoglobin localization to intercalated discs is preserved in desmoglein 2 mutants at 2 weeks of age. Scatterplots of IF signal ratios (in arbitrary units; AU) of desmoplakin (Dsp) and N-cadherin (N-Cad), β-catenin (β-cat), desmoglein 2 (Dsg2), plakophilin 2 (Pkp2), or plakoglobin (Pg) in intercalated discs of 2-week-old wild-type (wt; $n = 4$) and desmoglein 2-mutant mice (mt; $n = 4$). The plots also show the inter-quartile range together with the median. Note that a signal reduction in the mutant animals is only detectable for desmoglein 2 ($P = 0.0286$). Representative images for each situation are provided in Supplementary material online, *Figures S2–S4* as specified in the lower part of the diagram.

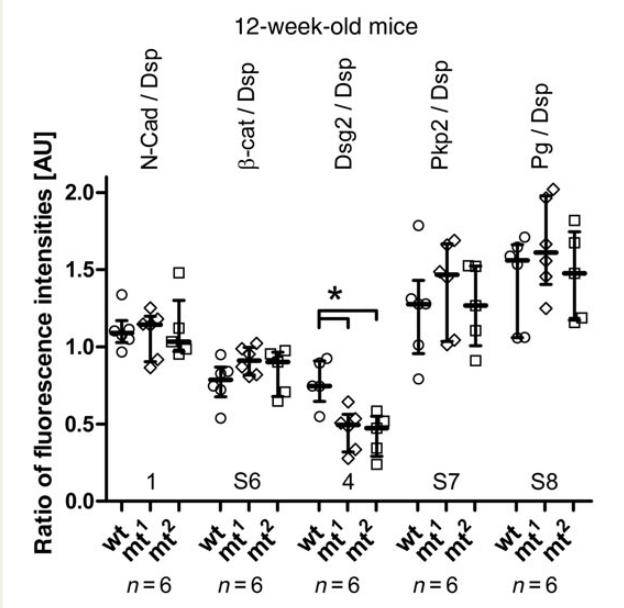

Figure 3 β-Catenin, plakophilin 2, and plakoglobin localization to intercalated discs is preserved in desmoglein 2 mutants at 12 weeks of age. Scatterplots of relative IF signal ratios (in arbitrary units; AU) measured in segmented intercalated discs of 12-week-old wild-type (wt) and desmoglein 2-mutant heart tissue (mt^1, remote area; mt^2, perilesional area; $n = 6$ in each instance). The plots also show the inter-quartile range together with the median. Ratios are shown for desmoplakin (Dsp) and N-cadherin (N-Cad), β-catenin (β-cat), desmoglein 2 (Dsg2), plakophilin 2 (Pkp2), or plakoglobin (Pg). A significant reduction in intercalated disc localization is only detectable for desmoglein 2 in the mutant ($P = 0.015$). Representative images for each situation are provided in *Figures 1* and *4* and Supplementary material online, *Figures S6–S8* as specified in the lower part of the diagram.

only very little unspecific signal in some instances. The fluorescence intensities were then determined in the segmented areas using the original recordings. For quantification, eight confocal fluorescence images were recorded from representative areas of each tissue sample. Each image encompassed 10–30 intercalated discs. Images were prepared from four age-matched wild-type and four desmoglein 2-mutant cardiac tissue samples. All of these images were prepared in a single session to exclude possible differences in signal strength because of hard ware variability. The analyses revealed no detectable difference in the ratios of N-cadherin and desmoplakin between the mutant and wild type (*Figures 1* and *2*), highlighting their suitability as internal standards. The same was true for other fluorescent markers outside the intercalated disc, which, however, showed a much higher degree of variability in fluorescence intensity (see comparison of anti-histone H3 and anti-desmoplakin in Supplementary material online, *Figure S1*) and were therefore not used in further experiments.

To assess the sensitivity of our method, we examined the level of mutant desmoglein 2 which was recently shown to be reduced in desmoglein 2-mutant mice.[4] As expected, a significant reduction in intercalated disc localization was observed in 2-week-old mice (*Figures 2* and right part of Supplementary material online, *Figure S2*).

Taken together, our IF-based method provides an objective, sensitive, and specific tool to examine differences in epitope abundance of intercalated disc components in cardiac tissue samples.

3.2 Armadillo proteins are efficiently targeted to intercalated discs of desmoglein 2-mutant mice independent of disease stage

Using the established methodology, we investigated the localization of the three major armadillo repeat-containing proteins of adhering junctions, i.e. plakoglobin, β-catenin, and plakophilin 2. We could not detect statistically significant alterations in intercalated disc localization for any of these proteins in 2-week-old desmoglein 2-mutant mice that did not present visible lesions (*Figure 2* and see Supplementary material online, *Figures S3* and *S4*).

To find out, whether redistribution of junctional proteins occurs at later disease stages, tissue samples were prepared from 12-week-old adult mice. By this time, either fibrotic lesions and/or diffuse fibrosis were detectable in all mutant animals. To account for possible local differences, images were acquired from perilesional areas and areas far away from fibrotic lesions. Again, no differences were detectable for any of the examined junctional proteins (*Figures 1* and *3* and see Supplementary material online, *Figures S6*, *S7* and *S8*) except for desmoglein 2, which was reduced in perilesional and remote areas (mt^2 and mt^1, respectively, in *Figures 3* and *4*).

Immunoblotting further showed that the levels of N-cadherin, β-catenin, plakophilin 2, desmoplakin, and plakoglobin did not differ

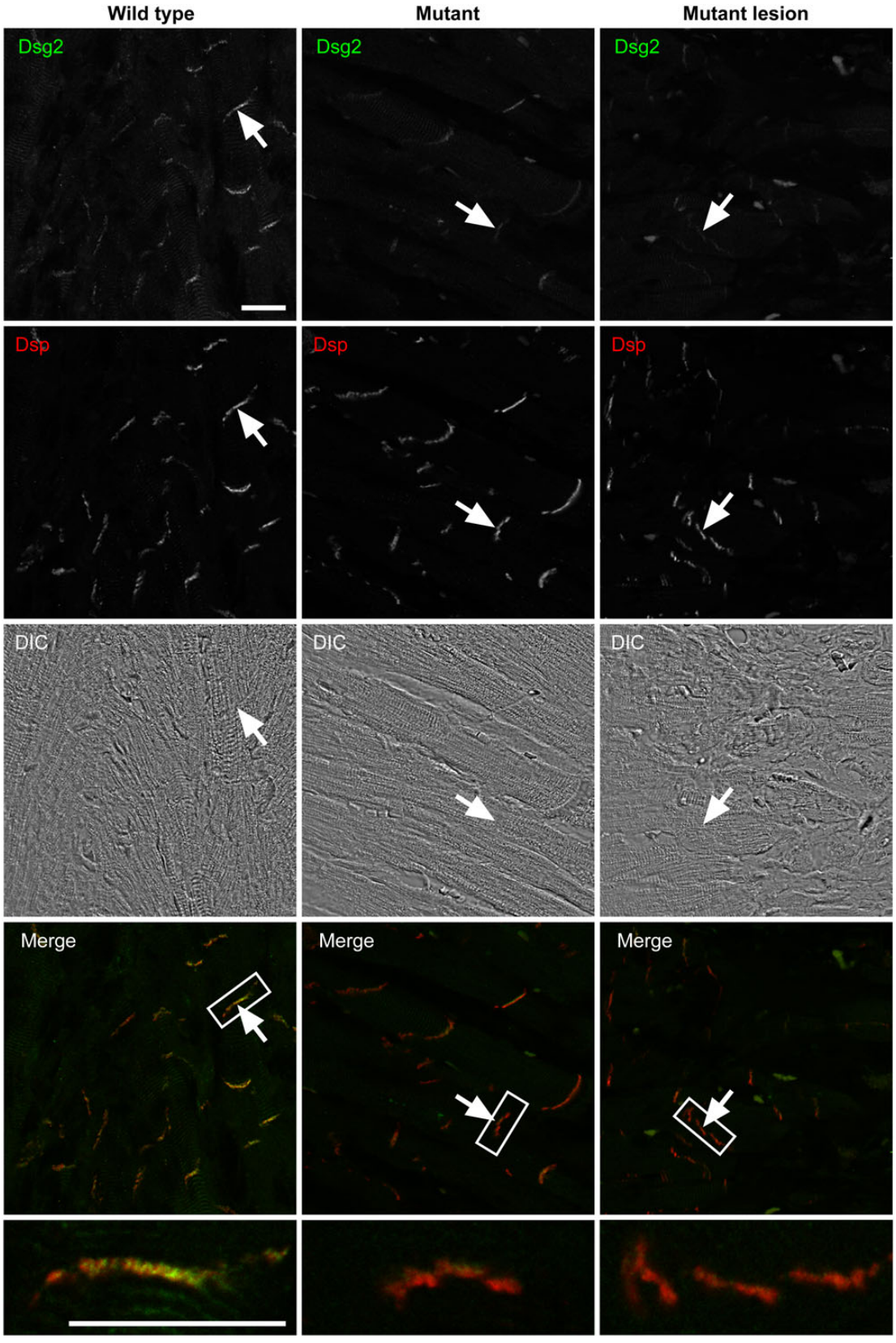

Figure 4 Both lesion and non-lesion areas have reduced desmoglein 2 in desmoglein 2 mutants at 12 weeks of age. Double IF microscopy [top rows; corresponding differential interference contrast images below (DIC)] detecting desmoglein 2 (Dsg2) with desmoplakin (Dsp) in 12-week-old wild-type and desmoglein 2-mutant hearts far away (mutant) or near a myocardial lesion (mutant lesion). The bottom rows show the merged images at the same and higher magnification (corresponding to arrow-marked boxed area). Note the reduction of desmoglein 2 at intercalated discs in the mutant. Size bars, 20 μm.

significantly between mutant and wild type, but that desmoglein 2 levels were significantly reduced in mutant mice (see Supplementary material online, *Figure S5*).

3.3 Altered intercalated disc localization of the armadillo proteins plakoglobin, plakophilin 2, and β-catenin is not a prerequisite for ARVC pathogenesis in humans

Next, we analysed whether differences exist in intercalated disc localization of armadillo proteins in the hearts of human ARVC patients. Tissue samples were obtained from end-stage heart failure patients (see Supplemental material online, *Figure S9*) with definite diagnosis of ARVC according to the revised task force criteria.[1] A first set of samples was taken from two patients with nonsense/frameshift mutations in the plakophilin 2 gene (*PKP2*; p.Q726X and p.D601E fs, respectively), one patient with the homozygous desmocollin 2 mutation *DCS2* p.Q638L fs, one patient with an unknown genetic defect, and one patient with a variant of unknown significance in the N-cadherin gene (*CDH2*; p.G85A) (*Table 1*). For comparison, tissue samples from five patients with clinically manifest dilative cardiomyopathy and from five donor hearts without known cardiac disease were examined. The results, which are summarized in *Figure 5* (examples in Supplementary material online, *Figures S10–14* and *S16*), show that the intercalated disc localization of N-cadherin, β-catenin, desmoglein 2, plakophilin 2, and plakoglobin (polyclonal antibodies) are unperturbed when normalized to anti-desmoplakin staining. Desmocollin 2, however, was considerably reduced in intercalated discs of the ARVC patient who carried the homozygous desmocollin 2 mutation (black square in *Figure 5*) but not in any of the other samples (see Supplementary material online, *Figure S14*). We regard this finding as a further indication of the sensitivity of our analyses. Along the same vein, the reduction of plakophilin 2 staining in patient samples 1 and 2 (black squares in *Figure 5*) may be explained by reduced plakophilin 2 expression, since the mutant alleles encode truncated plakophilins lacking the epitope recognized by antibody PP2–86.[33] Overall, our data do not provide evidence for consistently reduced armadillo proteins in intercalated discs of tissue samples from human ARVC patients.

3.4 Detection of reduced intercalated disc localization of plakoglobin is antibody dependent

Since different antibodies were used in the current study compared with previous studies, notably those that reported a reduced intercalated disc localization of plakoglobin,[15–17,19,21,36,37] we compared the immunoreactions of different plakoglobin antibodies. We selected four antibodies, namely (i) goat antibodies directed against a carboxy-terminal epitope that we had used for the above experiments, (ii) mouse mAb PG5.1 that also reacts with an epitope in the carboxy-terminal domain,[35] (iii) mouse mAb 15F11 that recognizes an epitope in the aminoterminus of plakoglobin[34] and had been used in most previous ARVC studies,[15,18,19,21,23,24] and (iv) guinea pig antibodies GP57 that react with the aminoterminal part of plakoglobin. Specificity of antibodies was assessed by immunoblotting of total cell extracts prepared from wild-type and mutant murine hearts (see Supplementary material online, *Figure S15*). All antibodies detected full-length plakoglobin. In addition, PG5.1 antibodies detected a ~53 kDa polypeptide and GP57 antibodies a ~70 kDa polypeptide.

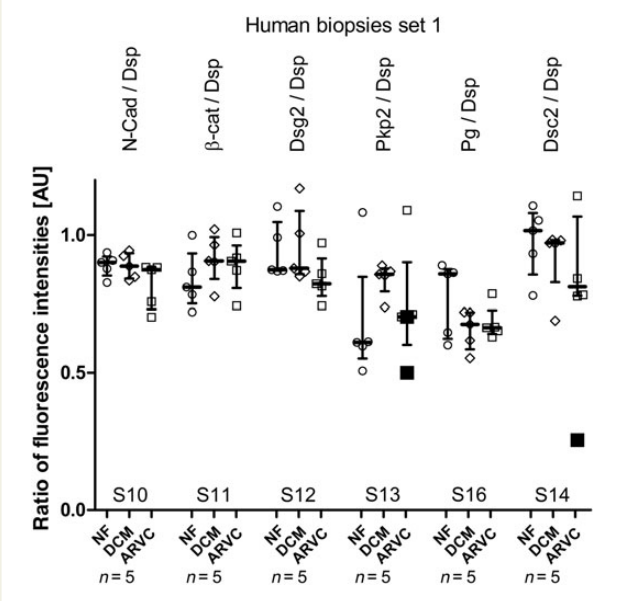

Figure 5 No evidence for reduced plakoglobin in intercalated discs is detectable in human ARVC samples using polyclonal goat antibodies. Scatterplots of relative IF signal ratios (in arbitrary units; AU) recorded in segmented intercalated disc regions of human heart tissues. Ratios between the immunosignals for desmoplakin (Dsp) and N-cadherin (N-Cad), β-catenin (β-cat), desmoglein 2 (Dsg2), plakophilin 2 (Pkp2), plakoglobin (Pg), or desmocollin 2 (Dsc2) are shown. Five samples were each obtained from healthy individuals without heart disease (NF; circles) and from patients with either dilative cardiomyopathy (DCM; diamonds) or ARVC (Patients 1–5 in *Table 1*; squares). The plots also show the inter-quartile range together with the median. Note that no differences in fluorescence intensity ratio could be observed between the different groups except for desmocollin 2. In this instance, a drastically reduced desmocollin 2 signal was observed in the sample from Patient 3 who was homozygous for a truncating desmocollin 2 mutation (black square). When the desmocollin 2 reactions of the other ARVC patients were compared with the control groups, no statistically significant difference could be detected. Black squares also denote the fluorescence intensity ratios of Pkp2 to Dsp measured in samples obtained from Patients 1 and 2 with plakophilin 2 mutations resulting in truncation of the epitope-carrying domain. Representative images for each situation are provided in Supplementary material online, *Figures S10–S14* and *S16* as specified in the lower part of the diagram.

Examination of hearts from 2-week-old desmoglein 2 mouse mutants revealed no differences in intercalated disc localization of plakoglobin using either the goat antibodies or PG5.1 (*Figures 6* and *7* and see Supplementary material online, *Figure S4*). In contrast, antibody 15F11 showed significantly reduced plakoglobin staining of intercalated discs in the mutant mouse hearts (*Figures 6* and *7*). Comparable differences were also found in the human tissue samples (*Figures 6* and see Supplementary material online, *Figures S16*, *S17* and *S18*). A slight, although not significant, reduction of plakoglobin 15F11 staining in intercalated discs was observed in human ARVC samples in comparison to normal tissue samples. Comparison of 15F11 immunoreactivity in intercalated discs of the ARVC samples to that in the DCM group, however, revealed a significant reduction. When 15F11 reactivity was normalized by N-cadherin staining instead of desmoplakin staining, a significant

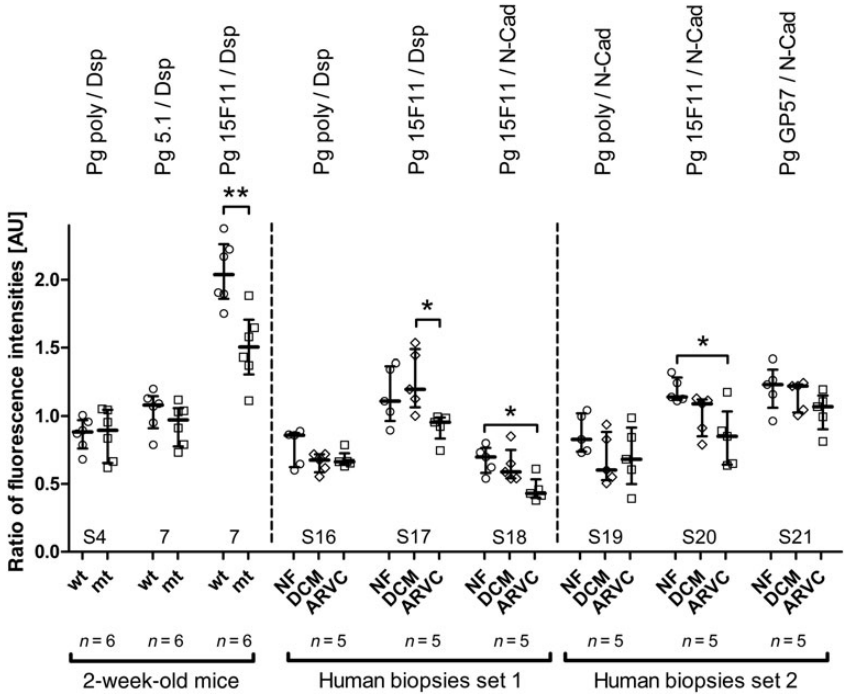

Figure 6 Only 15F11 antibodies detect a reduction in plakoglobin immunoreactivity in ARVC. Scatterplots of IF signal ratios of either desmoplakin (Dsp) or N-Cadherin (N-Cad) and plakoglobin using different antibodies that were measured in segmented intercalated discs of cardiac tissue samples obtained from wild-type (wt) and desmoglein 2-mutant mice (mt) and from humans without heart disease (NF), with DCM or ARVC (*Table 1*). The plots also show the inter-quartile range together with the median. Plakoglobin was detected with polyclonal goat antibodies (Pg poly) and monoclonal mouse antibody PG5.1, both of which react with a carboxyterminal epitope, with polyclonal guinea pig antibodies Pg GP57 reacting with the aminoterminal part of plakoglobin, with monoclonal mouse antibody Pg 15F11, which binds to a circumscribed epitope in the aminoterminal part of plakoglobin. Note that only the 15F11 reactivity is significantly reduced in murine mutant heart samples ($P = 0.0043$). In the first set of human samples, Pg 15F11 staining is also selectively reduced in the ARVC group with significant differences to the DCM group ($P = 0.024$) when normalized to desmoplakin immunoreactivity. Additionally, a significant reduction of Pg 15F11 immunoreactivity is found between the ARVC and NF groups in both sample sets when normalized to the N-cadherin immunoreactivity ($P = 0.0324$ for Set 1; $P = 0.0467$ for Set 2). Representative images for each situation are provided in *Figures 7*, Supplementary material online, *Figures S4* and *S16–S21* as specified in the lower part of the diagram.

reduction in ARVC samples was observed in comparison to samples from individuals without heart disease and a slight decrease in comparison to samples from patients with DCM.

To further corroborate these results, another set of five ARVC tissue samples (details in *Table 1*) was examined in comparison to samples from non-failing hearts and diseased hearts with DCM. Again, only 15F11 antibodies detected a reduction in immunoreactivity in ARVC samples, while the polyclonal goat and guinea pig antibodies did not (*Figures 6* and see Supplementary material online, *Figures S19–21*).

Taken together, our observations show that only antibodies directed against the 15F11-specific epitope detect differences in intercalated disc localization of plakoglobin in desmoglein 2-mutant murine and human ARVC hearts while antibodies directed at other parts of the molecule do not.

4. Discussion

The fact that mutations in all desmosomal protein-encoding genes expressed in heart have been identified in cases of ARVC can be taken as a strong indication for a common disease pathway in these instances. In the search for a common denominator, plakoglobin has been on centre stage. A key publication by Garcia-Gras *et al.*,[25] proposed that nuclear enrichment of plakoglobin initiates ARVC pathogenesis through suppression of canonical Wnt/β-catenin signalling in the nucleus. Evidence for this hypothesis has been presented in several subsequent studies in transgenic mice until recently.[27,38] Support for this unifying concept was further provided by the observation of reduced plakoglobin levels at intercalated discs in human ARVC patients carrying different mutations of desmosomal and non-desmosomal genes.[15]

The results of our current study, however, show that reduced plakoglobin at intercalated discs is not a prerequisite for the development of an ARVC phenotype. Normal plakoglobin distribution was detected in a murine model of ARVC both at early and late disease stages and in human ARVC patients. Comparison of several plakoglobin antibodies further revealed that the previously observed reduction of plakoglobin immunostaining in intercalated discs may be attributed to selective masking of the epitope recognized by Pg 15F11 antibody rather than protein mislocalization. In accordance, increased plakoglobin staining in other cell compartments including the nucleus has not been reported in any of the murine models or in human ARVC patients to date. Furthermore, the observed down-regulation of the wnt signalling target genes c-myc, CTGF, and cyclin D1 upon nuclear plakoglobin accumulation[25,27] are in stark contrast to the observed up-regulation of these mRNAs in desmoglein 2-mutant mice.[4,39] In support, recently

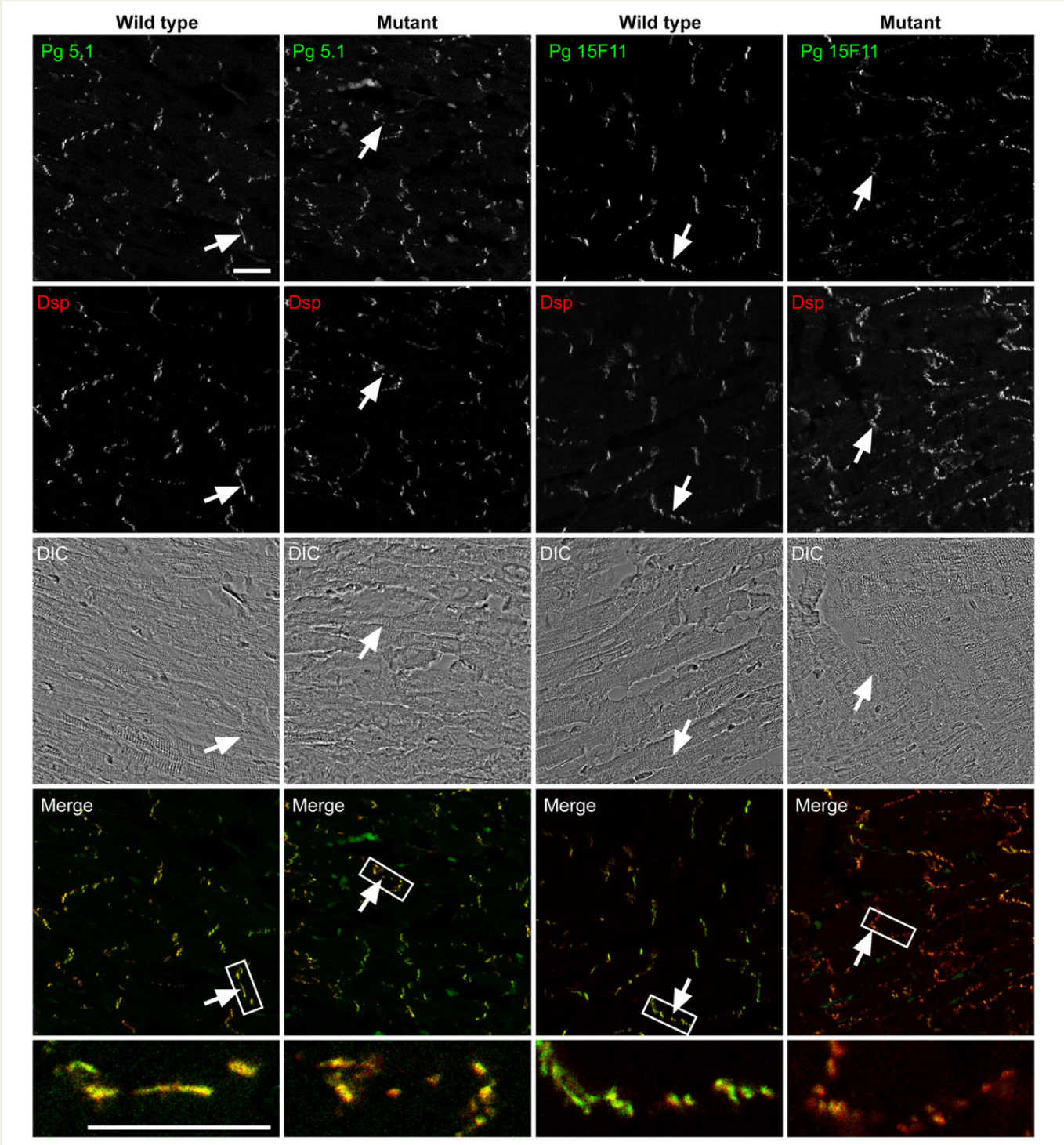

Figure 7 15F11 but not PG5.1 antibodies show reduced plakoglobin in desmoglein 2 mutants at 2 weeks. Double IF microscopy (top rows) and corresponding differential interference contrast images below (DIC) detecting plakoglobin either with antibody Pg 5.1 or with Pg 15F11 together with desmoplakin (Dsp) in 2-week-old wild-type and desmoglein 2-mutant hearts. Merged fluorescence images are shown at low and high magnification (corresponding to arrow-marked boxed area) at the bottom. Note the slightly reduced Pg 15F11 fluorescence intensity in the intercalated discs of mutant samples. Size bars, 20 μm.

published transcriptome analyses of 6 ARVC patients vs. 6 healthy controls[40] revealed a significant up-regulation of CTGF and cyclin D1 and no changes in c-myc expression (data taken from NCBI GEO-database accession number GSE29819).

The observed differences in antigenicity point to conformational changes and/or altered molecular interactions of plakoglobin in the diseased tissue. It will be interesting to learn how these apparently common alterations in ARVC affect plakoglobin function and

whether they are related to ARVC pathogenesis. It is attractive to speculate that the reduction and mutation of desmoglein 2 in our mouse model lead to alteration of the conformation of plakoglobin and/or liberate plakoglobin binding sites. These sites would, in turn, be available for either intramolecular or intermolecular interactions within the intercalated disc resulting in masking of the circumscribed epitope recognized by antibody 15F11.[34] This scenario is not without precedence: it has been shown that desmogleins compete with α-catenin for the same aminoterminal binding site of plakoglobin[35,41] and with classical cadherins for other binding sites.[35,42,43] Similar effects may occur in other desmosome-related forms of ARVC given the association of plakoglobin with all major desmosomal components.[44,45] The outcome in all instances could be that signalling and/or mechanical linker functions of intercalated disc-localized plakoglobin are altered.

Another surprising outcome of our study is that the reduction of desmosomal cadherins does not affect the localization of any major desmosomal plaque proteins, i.e. besides plakoglobin, desmoplakin, and plakophilin 2. The same was true for ARVC patients carrying other mutations. Furthermore, we cannot detect obvious alterations in desmin intermediate filament distribution (data not shown). These findings are in agreement with observations by others,[23,24] although contrasting results have been reported elsewhere.[16]

Taken together, our findings suggest that ARVC is either a much more heterogeneous disease than hitherto assumed with multiple pathogenic mechanisms or that the observed alterations in signalling are not triggered by relocalization of desmosomal and non-desmosomal arm-repeat proteins but by other cues. Given the frequent involvement of desmosomal proteins in ARVC, we favour the second possibility. Protein modification may be induced which do not result in redistribution but in altered protein interactions. Thus, while β-catenin was reported to be properly localized to intercalated discs in heterozygous plakoglobin-deficient mice,[46] a reduction in β-catenin phosphorylation implicating altered PI3K-AKT signalling was reported for mice with a cardiac tissue-restricted depletion of plakoglobin.[47] Recent publications point to involvement of other pathways besides canonical wnt signalling, most notably the Hippo pathway.[48,49] In addition, desmosome-specific dysfunctions such as compromised mechanotransduction, mechanosensation, or vesicle trafficking may either by themselves or through resulting increase in mechanical stress induce these pathways as has been shown for the induction of the MRTF/SRF pathway.[50]

Supplementary material

Supplementary material is available at *Cardiovascular Research* online.

Acknowledgements

We thank Marina Lürkens-Weber and Claudia Schmitz for expert technical assistance.

Conflict of interest: none declared.

Funding

This work was supported by the German Research Council (LE 566/11–1), the Interdisciplinary Center for Clinical Research (IZKF) within the Faculty of Medicine at RWTH Aachen University, the Erich & Hanna Klessmann-Foundation, and the Heart Valve Bank of the University Hospital Rotterdam (control tissue of rejected donor hearts).

References

1. Marcus FI, McKenna WJ, Sherrill D, Basso C, Bauce B, Bluemke DA, Calkins H, Corrado D, Cox MG, Daubert JP, Fontaine G, Gear K, Hauer R, Nava A, Picard MH, Protonotarios N, Saffitz JE, Sanborn DM, Steinberg JS, Tandri H, Thiene G, Towbin JA, Tsatsopoulou A, Wichter T, Zareba W. Diagnosis of arrhythmogenic right ventricular cardiomyopathy/dysplasia: proposed modification of the Task Force Criteria. *Eur Heart J* 2010;**31**:806–814.
2. Saguner AM, Brunckhorst C, Duru F. Arrhythmogenic ventricular cardiomyopathy: a paradigm shift from right to biventricular disease. *World J Cardiol* 2014;**6**:154–174.
3. Kant S, Krull P, Eisner S, Leube RE, Krusche CA. Histological and ultrastructural abnormalities in murine desmoglein 2-mutant hearts. *Cell Tissue Res* 2012;**348**:249–259.
4. Krusche CA, Holthofer B, Hofe V, van de Sandt AM, Eshkind L, Bockamp E, Merx MW, Kant S, Windoffer R, Leube RE. Desmoglein 2 mutant mice develop cardiac fibrosis and dilation. *Basic Res Cardiol* 2011;**106**:617–633.
5. Li D, Liu Y, Maruyama M, Zhu W, Chen H, Zhang W, Reuter S, Lin SF, Haneline LS, Field LJ, Chen PS, Shou W. Restrictive loss of plakoglobin in cardiomyocytes leads to arrhythmogenic cardiomyopathy. *Hum Mol Genet* 2011;**20**:4582–4596.
6. Pilichou K, Remme CA, Basso C, Campian ME, Rizzo S, Barnett P, Scicluna BP, Bauce B, van den Hoff MJ, de Bakker JM, Tan HL, Valente M, Nava A, Wilde AA, Moorman AF, Thiene G, Bezzina CR. Myocyte necrosis underlies progressive myocardial dystrophy in mouse dsg2-related arrhythmogenic right ventricular cardiomyopathy. *J Exp Med* 2009;**206**:1787–1802.
7. Gerull B, Heuser A, Wichter T, Paul M, Basson CT, McDermott DA, Lerman BB, Markowitz SM, Ellinor PT, MacRae CA, Peters S, Grossmann KS, Drenckhahn J, Michely B, Sasse-Klaassen S, Birchmeier W, Dietz R, Breithardt G, Schulze-Bahr E, Thierfelder L. Mutations in the desmosomal protein plakophilin-2 are common in arrhythmogenic right ventricular cardiomyopathy. *Nat Genet* 2004;**36**:1162–1164.
8. Basso C, Corrado D, Bauce B, Thiene G. Arrhythmogenic right ventricular cardiomyopathy. *Circ Arrhythm Electrophysiol* 2012;**5**:1233–1246.
9. Bao JR, Wang JZ, Yao Y, Wang YL, Fan XH, Sun K, Zhang S, Hui RT, Song L. Screening of pathogenic genes in Chinese patients with arrhythmogenic right ventricular cardiomyopathy. *Chin Med J (Engl)* 2013;**126**:4238–4241.
10. Fressart V, Duthoit G, Donal E, Probst V, Deharo JC, Chevalier P, Klug D, Dubourg O, Delacretaz E, Cosnay P, Scanu P, Extramiana F, Keller D, Hidden-Lucet F, Simon F, Bessirard V, Roux-Buisson N, Hebert JL, Azarine A, Casset-Senon D, Rouzet F, Lecarpentier Y, Fontaine G, Coirault C, Frank R, Hainque B, Charron P. Desmosomal gene analysis in arrhythmogenic right ventricular dysplasia/cardiomyopathy: spectrum of mutations and clinical impact in practice. *Europace* 2010;**12**:861–868.
11. Romero J, Mejia-Lopez E, Manrique C, Lucariello R. Arrhythmogenic right ventricular cardiomyopathy (ARVC/D): a systematic literature review. *Clin Med Insights Cardiol* 2013;**7**:97–114.
12. Otten E, Asimaki A, Maass A, van Langen IM, van der Wal A, de Jonge N, van den Berg MP, Saffitz JE, Wilde AA, Jongbloed JD, van Tintelen JP. Desmin mutations as a cause of right ventricular heart failure affect the intercalated disks. *Heart Rhythm* 2010;**7**:1058–1064.
13. Rickelt S, Pieperhoff S. Mutations with pathogenic potential in proteins located in or at the composite junctions of the intercalated disk connecting mammalian cardiomyocytes: a reference thesaurus for arrhythmogenic cardiomyopathies and for Naxos and Carvajal diseases. *Cell Tissue Res* 2012;**348**:325–333.
14. van der Zwaag PA, van Rijsingen IA, Asimaki A, Jongbloed JD, van Veldhuisen DJ, Wiesfeld AC, Cox MG, van Lochem LT, de Boer RA, Hofstra RM, Christiaans I, van Spaendonck-Zwarts KY, Lekanne dit Deprez RH, Judge DP, Calkins H, Suurmeijer AJ, Hauer RN, Saffitz JE, Wilde AA, van den Berg MP, van Tintelen JP. Phospholamban R14del mutation in patients diagnosed with dilated cardiomyopathy or arrhythmogenic right ventricular cardiomyopathy: evidence supporting the concept of arrhythmogenic cardiomyopathy. *Eur J Heart Fail* 2012;**14**:1199–1207.
15. Asimaki A, Tandri H, Huang H, Halushka MK, Gautam S, Basso C, Thiene G, Tsatsopoulou A, Protonotarios N, McKenna WJ, Calkins H, Saffitz JE. A new diagnostic test for arrhythmogenic right ventricular cardiomyopathy. *N Engl J Med* 2009;**360**:1075–1084.
16. Gehmlich K, Asimaki A, Cahill TJ, Ehler E, Syrris P, Zachara E, Re F, Avella A, Monserrat L, Saffitz JE, McKenna WJ. Novel missense mutations in exon 15 of desmoglein-2: role of the intracellular cadherin segment in arrhythmogenic right ventricular cardiomyopathy? *Heart Rhythm* 2010;**7**:1446–1453.
17. Gehmlich K, Syrris P, Reimann M, Asimaki A, Ehler E, Evans A, Quarta G, Pantazis A, Saffitz JE, McKenna WJ. Molecular changes in the heart of a severe case of arrhythmogenic right ventricular cardiomyopathy caused by a desmoglein-2 null allele. *Cardiovasc Pathol* 2012;**21**:275–282.
18. Noorman M, Hakim S, Kessler E, Groeneweg JA, Cox MG, Asimaki A, van Rijen HV, van Stuijvenberg L, Chkourko H, van der Heyden MA, Vos MA, de Jonge N, van der Smagt JJ, Dooijes D, Vink A, de Weger RA, Varro A, de Bakker JM, Saffitz JE, Hund TJ, Mohler PJ, Delmar M, Hauer RN, van Veen TA. Remodeling of the cardiac sodium channel, connexin43, and plakoglobin at the intercalated disk in patients with arrhythmogenic cardiomyopathy. *Heart Rhythm* 2013;**10**:412–419.
19. Munkholm J, Christensen AH, Svendsen JH, Andersen CB. Usefulness of immunostaining for plakoglobin as a diagnostic marker of arrhythmogenic right ventricular cardiomyopathy. *Am J Cardiol* 2012;**109**:272–275.

20. Kwon YS, Park TI, Cho Y, Bae MH, Kim S. Clinical usefulness of immunohistochemistry for plakoglobin, N-cadherin, and connexin-43 in the diagnosis of arrhythmogenic right ventricular cardiomyopathy. *Int J Clin Exp Pathol* 2013;**6**:2928–2935.
21. Ermakov S, Ursell PC, Johnson CJ, Meadows A, Zhao S, Marcus GM, Scheinman M. Plakoglobin immunolocalization as a diagnostic test for arrhythmogenic right ventricular cardiomyopathy. *Pacing Clin Electrophysiol* 2014;**37**:1708–1716.
22. Asimaki A, Tandri H, Duffy ER, Winterfield JR, Mackey-Bojack S, Picken MM, Cooper LT, Wilber DJ, Marcus FI, Basso C, Thiene G, Tsatsopoulou A, Protonotarios N, Stevenson WG, McKenna WJ, Gautam S, Remick DG, Calkins H, Saffitz JE. Altered desmosomal proteins in granulomatous myocarditis and potential pathogenic links to arrhythmogenic right ventricular cardiomyopathy. *Circ Arrhythm Electrophysiol* 2011;**4**:743–752.
23. Vite A, Gandjbakhch E, Prost C, Fressart V, Fouret P, Neyroud N, Gary F, Donal E, Varnous S, Fontaine G, Fornes P, Hidden-Lucet F, Komajda M, Charron P, Villard E. Desmosomal cadherins are decreased in explanted arrhythmogenic right ventricular dysplasia/cardiomyopathy patient hearts. *PLoS One* 2013;**8**:e75082.
24. Tavora F, Zhang M, Cresswell N, Li L, Fowler D, Franco M, Burke A. Quantitative immunohistochemistry of desmosomal proteins (plakoglobin, desmoplakin and plakophilin), connexin-43, and N-cadherin in arrhythmogenic cardiomyopathy: an autopsy study. *Open Cardiovasc Med J* 2013;**7**:28–35.
25. Garcia-Gras E, Lombardi R, Giocondo MJ, Willerson JT, Schneider MD, Khoury DS, Marian AJ. Suppression of canonical Wnt/beta-catenin signaling by nuclear plakoglobin recapitulates phenotype of arrhythmogenic right ventricular cardiomyopathy. *J Clin Invest* 2006;**116**:2012–2021.
26. Asimaki A, Saffitz JE. Remodeling of cell-cell junctions in arrhythmogenic cardiomyopathy. *Cell Commun Adhes* 2014;**21**:13–23.
27. Lombardi R, da Graca Cabreira-Hansen M, Bell A, Fromm RR, Willerson JT, Marian AJ. Nuclear plakoglobin is essential for differentiation of cardiac progenitor cells to adipocytes in arrhythmogenic right ventricular cardiomyopathy. *Circ Res* 2011;**109**:1342–1353.
28. Awad MM, Calkins H, Judge DP. Mechanisms of disease: molecular genetics of arrhythmogenic right ventricular dysplasia/cardiomyopathy. *Nat Clin Pract Cardiovasc Med* 2008;**5**:258–267.
29. Klauke B, Kossmann S, Gaertner A, Brand K, Stork I, Brodehl A, Dieding M, Walhorn V, Anselmetti D, Gerdes D, Bohms B, Schulz U, Zu Knyphausen E, Vorgerd M, Gummert J, Milting H. De novo desmin-mutation N116S is associated with arrhythmogenic right ventricular cardiomyopathy. *Hum Mol Genet* 2010;**19**:4595–4607.
30. Brodehl A, Hedde PN, Dieding M, Fatima A, Walhorn V, Gayda S, Saric T, Klauke B, Gummert J, Anselmetti D, Heilemann M, Nienhaus GU, Milting H. Dual color photoactivation localization microscopy of cardiomyopathy-associated desmin mutants. *J Biol Chem* 2012;**287**:16047–16057.
31. Groeneweg JA, van der Zwaag PA, Olde Nordkamp LR, Bikker H, Jongbloed JD, Jongbloed R, Wiesfeld AC, Cox MG, van der Heijden JF, Atsma DE, de Boer K, Doevendans PA, Vink A, van Veen TA, Dooijes D, van den Berg MP, Wilde AA, van Tintelen JP, Hauer RN. Arrhythmogenic right ventricular dysplasia/cardiomyopathy according to revised 2010 task force criteria with inclusion of non-desmosomal phospholamban mutation carriers. *Am J Cardiol* 2013;**112**:1197–1206.
32. Schlegel N, Meir M, Heupel WM, Holthofer B, Leube RE, Waschke J. Desmoglein 2-mediated adhesion is required for intestinal epithelial barrier integrity. *Am J Physiol Gastrointest Liver Physiol* 2010;**298**:G774–G783.
33. Mertens C, Kuhn C, Franke WW. Plakophilins 2a and 2b: constitutive proteins of dual location in the karyoplasm and the desmosomal plaque. *J Cell Biol* 1996;**135**:1009–1025.
34. Sacco PA, McGranahan TM, Wheelock MJ, Johnson KR. Identification of plakoglobin domains required for association with N-cadherin and alpha-catenin. *J Biol Chem* 1995;**270**:20201–6.
35. Wahl JK, Sacco PA, McGranahan-Sadler TM, Sauppe LM, Wheelock MJ, Johnson KR. Plakoglobin domains that define its association with the desmosomal cadherins and the classical cadherins: identification of unique and shared domains. *J Cell Sci* 1996;**109**(Pt 5):1143–1154.
36. Noorman M, Hakim S, Asimaki A, Vreeker A, van Rijen HV, van der Heyden MA, de Jonge N, de Weger RA, Hauer RN, Saffitz JE, van Veen TA. Reduced plakoglobin immunoreactivity in arrhythmogenic cardiomyopathy: methodological considerations. *Cardiovasc Pathol* 2013;**22**:314–318.
37. Munkholm J, Andersen CB, Ottesen GL. Plakoglobin: a diagnostic marker of arrhythmogenic right ventricular cardiomyopathy in forensic pathology? *Forensic Sci Med Pathol* 2015;**11**:47–52.
38. Lombardi R, Dong J, Rodriguez G, Bell A, Leung TK, Schwartz RJ, Willerson JT, Brugada R, Marian AJ. Genetic fate mapping identifies second heart field progenitor cells as a source of adipocytes in arrhythmogenic right ventricular cardiomyopathy. *Circ Res* 2009;**104**:1076–1084.
39. Hofe V. *Murine Desmoglein 2-Mutanten als Tiermodell zur Untersuchung der Arrhythmogenen Rechtsventrikulären Kardiomyopathie*. VVB Laufersweiler Verlag: Gießen; 2009. p1–124.
40. Gaertner A, Schwientek P, Ellinghaus P, Summer H, Golz S, Kassner A, Schulz U, Gummert J, Milting H. Myocardial transcriptome analysis of human arrhythmogenic right ventricular cardiomyopathy. *Physiol Genomics* 2012;**44**:99–109.
41. Ozawa M, Terada H, Pedraza C. The fourth armadillo repeat of plakoglobin (gamma-catenin) is required for its high affinity binding to the cytoplasmic domains of E-cadherin and desmosomal cadherin Dsg2, and the tumor suppressor APC protein. *J Biochem* 1995;**118**:1077–1082.
42. Al-Jassar C, Bikker H, Overduin M, Chidgey M. Mechanistic basis of desmosome-targeted diseases. *J Mol Biol* 2013;**425**:4006–4022.
43. Choi HJ, Gross JC, Pokutta S, Weis WI. Interactions of plakoglobin and beta-catenin with desmosomal cadherins: basis of selective exclusion of alpha- and beta-catenin from desmosomes. *J Biol Chem* 2009;**284**:31776–31788.
44. Holthofer B, Windoffer R, Troyanovsky S, Leube RE. Structure and function of desmosomes. *Int Rev Cytol* 2007;**264**:65–163.
45. Swope D, Li J, Radice GL. Beyond cell adhesion: the role of armadillo proteins in the heart. *Cell Signal* 2013;**25**:93–100.
46. Fabritz L, Hoogendijk MG, Scicluna BP, van Amersfoorth SC, Fortmueller L, Wolf S, Laakmann S, Kreienkamp N, Piccini I, Breithardt G, Noppinger PR, Witt H, Ebnet K, Wichter T, Levkau B, Franke WW, Pieperhoff S, de Bakker JM, Coronel R, Kirchhof P. Load-reducing therapy prevents development of arrhythmogenic right ventricular cardiomyopathy in plakoglobin-deficient mice. *J Am Coll Cardiol* 2011;**57**:740–750.
47. Li J, Swope D, Raess N, Cheng L, Muller EJ, Radice GL. Cardiac tissue-restricted deletion of plakoglobin results in progressive cardiomyopathy and activation of {beta}-catenin signaling. *Mol Cell Biol* 2011;**31**:1134–1144.
48. Chen SN, Gurha P, Lombardi R, Ruggiero A, Willerson JT, Marian AJ. The hippo pathway is activated and is a causal mechanism for adipogenesis in arrhythmogenic cardiomyopathy. *Circ Res* 2014;**114**:454–468.
49. Hu Y, Pu WT. Hippo activation in arrhythmogenic cardiomyopathy. *Circ Res* 2014;**114**:402–405.
50. Ho CY, Jaalouk DE, Vartiainen MK, Lammerding J. Lamin A/C and emerin regulate MKL1-SRF activity by modulating actin dynamics. *Nature* 2013;**497**:507–511.